BioCore Exploring Scientific Community

International Journal of Pharma Sciences and Scientific Research

Research Article ISSN 2471-6782

A Proposed Therapeutic Combination of Anti-VEGF Nanocarriers with Mesenchymal Stromal Cells on an Innovative Cellular Model able to Evaluate Medicines against Retinal Vein Occlusion

Eleni Gounari[1,2,6*], Stavroula Nanaki[3], Anastasia Komnenou[4], Evangelia Kofidou[4,5], Vassileios Karampatakis[6], Dimitrios Bikiaris[3], George Koliakos[1,2]

1) Department of Biochemistry, School of Medicine, Faculty of Health Sciences, Aristotle University of Thessaloniki, 54124 Thessaloniki, Greece
2) Biohellenika Biotechnology Company, Leoforos Georgikis Scholis 65, 57001, Thessaloniki, Greece
3) Department of Chemistry, Laboratory of Polymer Chemistry and Technology, Aristotle University of Thessaloniki, 54124 Thessaloniki, Greece
4) School of Veterinary Medicine, Faculty of Health Sciences, Aristotle University of e)Thessaloniki, St, Voutyra 11, 54627 Thessaloniki, Greece
5)Department of Biological Applications & Technology, University of Ioannina, 45110 Ioannina, Greece
6) Laboratory of Experimental Ophthalmology, School of Medicine, Faculty of Health Sciences, Aristotle University of Thessaloniki, 54124 Thessaloniki, Greece

Abstract

In recent years, anti-angiogenic therapeutic agents (anti-VEGF) have contributed to the treatment of retinal vein occlusion (RVO). At the same time, Mesenchymal Stromal Cells (MSCs) secretory agents protect the ganglion cells, limiting eye degeneration. An *in vitro* model to evaluate medicines that may be effective in RVO therapy is missing. In an attempt to evaluate such a model, MEK kinase inhibitor-PD0325901 was used to induce the expression of EPCR (Endothelial Protein C Receptor) on HUVEC (Human Umbilical Cord Endothelial Cell) culture. Anti-VEGF encapsulated in thiolated chitosan (ThioCHI) nanoparticles, MSCs and a combination of these was applied to the cultures and their effect was monitored. Net nanoparticles of CHI and ThioCHI were prepared by ionic gelation technique while ThioCHI was selected as polymeric matrix for anti-VEGF encapsulation. Their full characterization was followed using Fourier-transform infrared spectroscopy, Differential scanning calorimetry and X-ray diffraction. MSCs were prepared from human adipose tissue liposuction cultured up to five passages. Following 24-hour exposure of HUVEC to PD0325901, the effect of anti-VEGF nanoparticles, MSCs, and a combination of these was assessed by quantifying the secreted EPCR and time-controlled anti-VEGF release using a commercial ELISA assay. The modified prepared nanoparticles showed no cytotoxic effect while antibody release was constant for 8 days. The abnormal EPCR levels were statistically significantly reduced after 24 and 48 hours following exposure of the abnormal endothelium either to the anti-VEGF nanoparticles or to MSCs. A combination of both agents was more effective than either agent separately on 24 hours. The expression of EPCR on PD0325901 induced HUVEC cultures may be used as a novel *in vitro*-RVO simulation model to test the efficacy of pharmaceuticals and other therapeutics, on RVO, reducing the animal cost for such experiments. Using this model anti-VEGF ThioCHI nanoparticles, MSCs and a combination of these agents have been positively evaluated.

Keywords: Retinal Vein Occlusion, anti-VEGF, Mesenchymal Stromal Cells, Chitosan, Thiolated chitosan, Nanoparticles

Corresponding author: Eleni Gounari

Biohellenika Biotechnology Company, Leoforos Georgikis Scholis 65, 57001, Thessaloniki, Greece. Tel No: +306979237737

E-mail: egounari@biohellenika.gr

Received: December 12, 2020
Accepted: December 21, 2020
Published: January 05, 2021

Abbreviations

AMD	age-related macular degeneration
ASCs	Adipose-derived Mesenchymal Stromal Cells
CHI	chitosan
DMEM	Dulbecco's Modified Eagle Medium
DSC	Differential scanning calorimetry
EPCR	Endothelial Protein C Receptor
FBS	fetal bovine serum
FT-IR	Fourier-transform infrared spectroscopy
HUVECs	Human Umbilical Cord Endothelial Cells
MSCs	Mesenchymal Stromal Cells
PBS	Phosphate Buffer Saline
PCR	polymerase chain reaction
RP	retinitis pigmentosa
RVO	retinal vein occlusion
ThioCHI	thiolated chitosan
VEGF	vascular endothelial growth factor
XRD	X-ray diffraction

Introduction

Retinal vein occlusion (RVO) is the second leading cause of retinal vascular disease after diabetic retinopathy (DR) (Klein et al., 2000). Although the pathogenesis of RVO is not yet fully understood, an important event is the intraluminal thrombus formation. The blockage of venous circulation causes an augmentation of intraluminal pressure in the capillaries, leading to hemorrhages and leakage of fluid within the retina, increase of interstitial pressure and a consequent reduction of retinal perfusion. Ischemia may develop resulting in secretion of vascular endothelial growth factor (VEGF) that causes further vascular leakage and retinal edema. Nowadays, intravitreal injections of anti-VEGF agents are administered aiming the improvement of the clinical outcomes in these patients (Campa et al., 2016). However, the advantages of anti-VEGF therapy can be diminished by the need for prolonged treatment with repeated intravitreal injections, which can cause severe problems like endophthalmitis and retinal detachment (Farjo et al., 2010).

To overcome the above mentioned complications a slow constant anti-VEGF delivery means could be used. Nanoparticles have been recently used as drug and gene delivery systems. Their main characteristic is the ability to target and efficiently deliver the incorporated substances with reduced side effects to the patient. Due to its properties; biocompatibility and biodegradability and no toxic effect, chitosan is one of the most studied polymer in medical, biomedical and pharmaceutical applications (Xu et al., 2003; Zhao et al., 2011). In order to enhance its mucoadhesiveness, it is proposed the modification of its structure with thiol groups which acts as cell receptors and facilitate cell adhesion, proliferation and differentiation (Senni et al., 2011; Xian et al., 2010). Chitosan nanoparticles have already been studied as drug delivery systems, essential oil encapsulation and in water purification systems. Antibodies delivery constitutes a new area for chitosan and its analog nanoparticles to be used.

An other promising therapeutic approach for RVO may also be the application of mesenchymal stromal cell (MSCs). Following recent developments in the field of regenerative medicine, MSC therapies have begun to be widely used for various forms of retinopathy (Rajashekhar, 2014). Recent studies show that the functional action of MSCs is related to secretory factors that protect the ganglion cells, regenerating the axons in the optic nerve, limiting further degeneration of the eye (Balmer et al., 2015; Mead et al., 2015). MSCs have been shown to present neuroprotective effects on degenerated retinal cells, which could be associated with delaying or even stopping of uncontrolled cell death (Inoue et al., 2007; Park et al., 2016).

A variety of clinical trials are in the spotlight aiming the determination of the therapeutic potency of MSCs in common retinopathies such as DR, age-related macular degeneration (AMD), retinitis pigmentosa (RP) and RVO (Rajashekhar, 2014; Balmer et al., 2015; Park et al., 2016; Xu et al., Rajashekhar et al., 2014; Bharti et al., 2014). The most widely used MSC are Adipose-derived Mesenchymal Stromal Cells (ASCs) that can be easily isolated from adipose tissue obtained by the minimally invasive procedure of liposuction.

An *in vitro* RVO model that could be used to test the above and other therapeutic approaches before animal pre-clinical experiments would be useful.

The inhibitor of MEK 1, 2 PD0325901 [N-(2,3-dihydroxy-propoxy)-3,4-difluoro-2-(2-fluoro-4-iodo-phenylamino)-benzamide], has been used in clinical trials for the treatment of solid tumors. However a complication of this therapy was RVO, described by the presence of cotton wool spots, hemorrhages, and vein occlusion. Based on this evidence, PD0325901 has been successfully applied to induce RVO following intravitreal administration to Dutch-Belted Rabbits providing thus a reliable pre-clinical experimental model of the disease (Huang et al., 2009). Rat retinal gene expression analysis has been performed to evaluate the potential mechanism(s) of PD0325901-mediated RVO. Preliminary results indicated the induction of soluble EPCR (Endothelial Protein C Receptor) expression in retinal endothelial cells, that may represent a critical factor for the development of RVO retinal damage (Huang et al., 2009). Accordingly, the *in vitro* influence on PD0325901 induced endothelium EPCR expression may be useful as an *in vitro* model for evaluating RVO therapeutics.

In the present study we used the above *in vitro* model to evaluate anti-VEGF releasing nanoparticles, ASCs and a combination of them as RVO therapeutics.

Materials and Methods

Materials and Reagents

Chitosan low molecular weight (50,000–190,000 Da, degree of deacetylation ≥ 75%) was purchased from Sigma-Aldrich. Thioglycolic acid (purum≥ 98%), N-Ethyl-N'-(3-dimethylaminopropyl) carbodiimide hydrochloride (EDAC • HCl) (purum ≥ 99%) and N-Hydroxysuccinimide (NHS) (purum 98%) were purchased from Sigma-Aldrich (St. Louis, MO, USA). Triphenylphosphate (TPP) (purum ≥ 99%) used as ionic cross linking agent was also supplied by Sigma-Aldrich. Phosphate Buffer Saline (PBS) was used as purchased from SigmaAldrich (St. Louis, MO, USA). Dulbecco's Modified Eagle Medium (DMEM) high glucose w/L glutamine w/sodium pyruvate, penicillin–streptomycin solution 100X, fetal bovine serum (FBS) and trypsin-EDTA 1x in PBS were purchased from BIOSERA (Kansascity, MO, USA), Osteogenesis, adipogenesis and chondrogenesis medium from GIBCO-BRL (Grand Island, NY, USA) while the (3-(4,5-dimethylthiazol-2-yl)-2,5-diphenyltetrazolium bromide) powder-MTT and DMSO from Sigma Aldrich (St. Louis, MO, USA).All other reagents were of analytical grade.

Synthesis of Thiolated Chitosan

Thiolated chitosan (TMC) was synthesized as previously reported (Nanaki et al., 2012) by a two-stage procedure reported by Zhu et al. (Zhu et al., 2012). In brief, 1 mL thioglycolic acid, 3.5 mg EDAC • HCl, and 2.0 mg NHS were inserted into a flask containing 2 mL DMF and the mixture was left under magnetic stirring overnight, resulting in the synthesis of NHS–ester as an intermediate product. In the second stage, 500 mg of low molecular weight chitosan was added to 4 mL hydrochloric solution, 1 M in concentration, and diluted with water to a final concentration of 2.5%. After that, NHS–ester was inserted dropwise into the chitosan solution, and the pH value was adjusted to 5. The resulting mixture was left under magnetic stirring overnight. Synthesized TMC was lyophilized and washed in a Soxhlet extractor until total elimination of unreacted monomers was achieved. After lyophilization, TMS appeared as a white, odorless solid with a fibrous structure.

Preparation of chitosan and thiolated chitosan nanoparticles

Net chitosan (CHI) and thiolated chitosan (ThioCHI) nanoparticles were prepared according to ionic gelation technique (Siafaka et al., 2015) with a slight modification. In brief, 200mg of CHI or ThioCHI was dissolved in 25mL of aqueous solution of acetic acid, 1% v/v in concentration. TPP aqueous solution, 2mg/mL in concentration and 25mL in volume, was inserted dropwise to the initial solution under magnetic stirring. The final ratio of CHI and ThioCHI to TPP was 4/1 w/w. The resulting mixture was left under magnetic stirring for 4 hours. Nanoparticles were formed due to interactions taking place between the negative groups of TPP and the positive charged groups

of CHI or ThioCHI. After 4 hours the pH was adjusted to 6.5-7 using aqueous solution of NaOH, 0.1M in concentration. Nanoparticles were isolated by lyophilization.

Analogous procedure was followed in order to prepare ThioCHI nanoparticles containing anti-VEGF. The polyclonal antibody-VEGF (Millipore, MA, USA) was inserted to the initial TPP aqueous solution with immediate adjustment of pH to 7 and all the other steps were kept the same.

Characterization of Prepared Nanoparticles

Fourier Transform-Infrared spectroscopy (FTIR) was used in order to reveal the successful bond formation. FT-IR spectra were obtained on a Perkin-Elmer FTIR spectrometer (Spectrum 1, Waltham, MA, USA) using pellets of nanoparticles dilutedin KBr. Infrared (IR) absorbance spectra were obtained between 450 and 4000 cm−1 at a resolution of4 cm−1 using 20 co-added scans. All spectra presented are normalized and baseline-corrected .

X-ray diffraction (XRD) was used in order to examine the crystallinity of CHI and ThioCHI before and after ionic gelation procedure. XRD analysis was performed on prepared nanoparticles over the5–45 2θ range, using a MiniFlex II diffractometer (Rigaku Co., Tokyo, Japan) with Bragg–Brentanogeometry (θ, 2θ) and Ni-filtered Cu Kα radiation (λ = 0.154 nm).

The morphology of the prepared microspheres was examined using a scanning electron microscope (SEM), type Jeol (JMS-840, Peabody, MA, USA). All the studied surfaces were coated with carbon black to avoid charging under the electron beam.

Cell lines

Isolation, culture and characterization of ASCs

Isolation of ASCs from adipose tissue was performed as we have previously described (Christodoulou et al., 2019). Briefly, after liposuction adipose tissue was suspended in PBS (1X, pH 7.4) after the consent of a healthy volunteer donor. Overnight digestion was performed with 5 mg collagenase type I per 10gr adipose tissue. One day after, the mixture was centrifuged at 850 g for 10 min. The pellet was resuspended in DMEM supplemented with 10 % FBS and 2 % Penicillin/Streptomycin and plated in culture flasks for 72 hours until cells' adherence to the plastic surface (37 °C incubation with 5 % CO_2). Cells were cultured for 2-3 passages while medium was changed every two days. Every cells' detachment was performed with 0.05 % Trypsin-EDTA.

Following media changes every 2-3 days and after 2-3 passages, the cells were characterized via flow cytometry. Briefly, upon detachment of cells and centrifugation at 800 g for 10 min, staining with monoclonal antibodies (mAbs) CD45-PerCP-Cy5, CD34-FITC, CD90-FITC, CD105-PE (BD Biosciences, SanJose, CA USA) was performed for 15 min in the absence of light and finally analysis in BD FACS Calibur (BD Biosciences, San Jose, CA USA).

The induction of differentiation towards osteocytes, adipocytes and chondrocytes was accomplished by introducing the appropriate medium in the culture for 25-30 days accompanied with media changes every 2-3 days. The success of differentiation was estimated with alizarin red, oil red and alcian blue staining respectively according to each differentiation medium manufacturer's instructions (Grand Island, NY, USA).

Isolation and characterization of HUVECs

HUVECs (Human Umbilical Vein Endothelial Cells) were isolated as we have previously described (Koliakou et al., 2019). In brief, 20-25 cm of umbilical cord near the placenta height, were collected and washed twice. The umbilical cord was placed in a plastic surface with its both ends cut transversely with a lancet, in order for the umbilical vein to be visible from both sides. After a mild restrain with the use of a pincher, a wash with PBS was performed 3 times from every side of the umbilical cord in the internal side of the vein. Subsequently, the one side of the vein was wide shut and in the one a PBS solution supplemented with 25 mg collagenase was added, preheated in 37°C for 30 min, until the complete filling of the vein cavity. After the closure of the open side, the umbilical cord was cautiously transferred in a preheated saline solution in 37°C for 15 min. Upon the complete incubation and the opening of the one side, the content of the vein was collected following mild massages and washes. After centrifugation, the pellet was resuspended in Endothelial cell growth (Lonza, Basel, Switzerland) and was subsequently plated in a T-25 culture flask and incubated in 37°C with 5% CO_2 with media changes every 2-3 days. The cells were then characterized via flow cytometry for the expression of the CD144 surface marker.

Induction of an *in vitro* PD0325901-mediated model of RVO

Aiming the exposure of an endothelial cell line to PD0325901, 5 x 103 HUVECs per well were seeded in 96-well plates and incubated until cellular attachment in the presence of Endothelial Cell Growth Medium. PD0325901(Cayman Chemical, Michigan, USA) dissolved and added to increased concentrations in cell culture supernatant for 24 h incubation.

In order to assess the cytotoxic impact of PD0325901 to HUVECs, cell supernatant was removed and MTT reactant was introduced in a ratio of 1:10 in culture medium for a 4 h incubation in 37°C with 5% CO_2. Upon the removal of the MTT, 200 μl/well of DMSO was introduced for one additional hour of incubation in the same conditions. The reduction of MTT was counted in 570 and 630 nm wave length (PerkinElmer, Massachusetts, USA).

To determine the effect of MEK inhibitor on the level of EPCR, a common RVO-related biomarker, HUVECs supernatant was collected, centrifuged at 16000 g for 5 min while the levels of secreted EPCR were measured using sEPCR ELISA kit (CUSABIO, Houston, USA).

VEGF transcriptional levels quantification with real-time PCR

Aiming the quantification of the expression levels of VEGF gene to the abnormal endothelium after 24h or 48h PD0325901 effect on it, real time polymerase chain reaction (PCR) with the use KAPA SYBR FAST one step qPCR Master Mix (2X) Kit was performed. Untreated or treated with toxic concentration HUVEC were detached by using 0.05% Trypsin-EDTA followed by RNA extraction procedure according to the manufacturer's instructions (Macherey– Nagel, Du ¨ren, Germany) and a subsequent RNA quantification in a NanoDrop ND-1000 UV–Vis Spectrophotometer. After a cautious primer design as well as HPLC Purification (Lab Supplies, Athens, Greece), Q-PCR for 10 ng of RNA template was performed, the results of which were analyzed by using ddCt algorithm for the analysis of the relative changes in gene expression.

Estimation of cytotoxicity effect of prepared nano--particles on ASCs

ASCs were exposed to both CHI and ThioCHI nanoparticles and the

MTT assay was carried out for 24 h as described above. Nanoparticles were added in the culture supernatants at five different concentrations: 0,1-1-5-10-20 mg/ml in DMEM. For the sterilization of the solutions, 0.22 μm filter units were used. Non-nanoparticles treated cells were used as a control group in the same number as the other groups.

Quantification of time-control release of anti-VEGF in culture

Upon sterilization with a 0.22μm filter, ThioCHI containing anti-VEGF nanoparticles dissolved in culture medium in the highest non-cytotoxic concentration. After ASCs seeding and development up to 50 % confluency on plastic surfaces, the nanoparticles' enriched solutions were added for further incubation. ASCs, plated to similar cellular density, remained in simple medium without nanoparticles as control condition. Aiming to quantify the time-control release of anti-VEGF in culture, within 8 days and for several time points supernatants from all tested groups were collected, centrifuged at 16000 g for 5 min while the levels of released anti-VEGF were measured using VEGF ELISA kit (CUSABIO, Houston, USA).

Estimation of the influence of nanoparticles, ASCs or their combination to the *in vitro* induced RVO model

Aiming the evaluation of the nanoparticles/ASCs combination's impact to the treated with PD0325901 HUVEC, semi-permeable transwell membrane systems were used as decribed below. 2 x 105 HUVECs were counted and plated per well in 24-well plates to be exposed to PD0325901 upon their attachment to the plastic surface according to the results of the referred to 2.6 section procedure. After the 24 h exposure to the MEK inhibitor for the development of the *in vitro* RVO model, cell culture inserts of 0.22μm pore size, were placed on the wells containing 5 x 103 ASCs/well only, ThioCHI/anti-VEGF nanoparticles or their combination. The co-culture systems were incubated in 37°C with 5% CO_2 while supernatant was selected, in different time points without medium change previously, and EPCR secreted levels were quantified using a commercial ELISA kit as previously described.

Statistical analysis

Data are presented as the mean ±SD and the Student's t-test (unpaired, two-tailed) was used for the two-group comparisons. Differences were considered statistically significant at a value of $p \leq 0.05$.

Results

Characterization of the prepared nanoparticles

Nanoparticles of CHI and ThioCHI were prepared by the well-established technique ionic gelation. According to it there is a bond formation between the anionic groups of chitosan chain, which are negatively churched, and the cationic groups of a salt, TPP in this case, which is positively charged. Bond formation leads to a stable matrix which is difficult to be destroyed but has swelling properties that makes them ideal for drug or antibodies delivery systems.

FT-IR was used in order to determine the bond formation CHI and ThioCHI with TPP. As can be observed in Fig. 1a chitosan showed all the characteristic peaks; a broad peak at the range 3000-3600 cm-1, owing to stretching vibrations of O-H bonds, as well as to the intramolecular bonds of polysaccharide chain. The peak at 2889cm-1is attributed to stretching vibrations of methylene groups. The absorption peaks at 1665and 1563cm−1are due to amideI –NH2 bending and the amide II. Shifts of the proper peaks were observed to net nanoparticles' FT-IR; i.e. at 2923, 1631 and 1589 cm-1 respectively indicating that bond formation was conducted.

FT-IR spectra of ThioCHI (Fig. 1b) showed all the characteristic peaks as referred in our previous study (Zhao et al., 2011); i.e. an amide bond at 1590 cm-1 and a peak at 2680 cm-1 owning to H-S bond. FT-IR spectra of prepared nanoparticles showed shifts compared to the spectra of ThioCHI ought to interactions took place between ThioCHI and TPP. Furthermore, new peaks are appeared to the spectra; a small peak at 1642cm-1 and another one at 813 cm-1, indicating bond formation between TPP and ThioCHI.

XRD was used in order to study the crystallinity before and after nanoparticles formation. As can be observed, CHI is a semi-crystalline polymer with a relative high broad peak showed at 19.4 deg and a smaller broad peak at 10.7 deg. TPP has high crystallinity. After nanoparticles formation net nanoparticles showed to have lower crystallinity with a small broad peak at 8.4 deg, a broad one at 22.5 deg and a very small broad at 30.7 deg, showing that crystal structure of chitosan was modified.

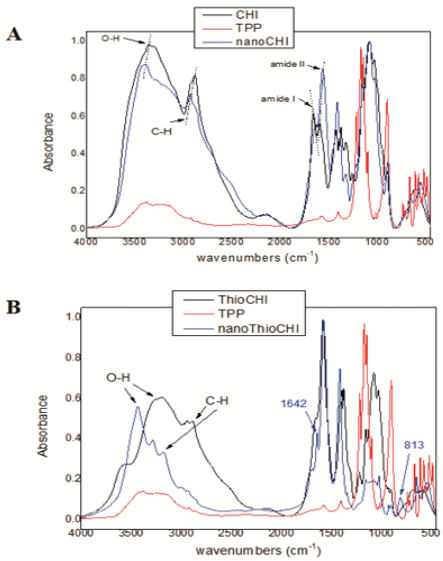

Fig. 1. FT-IR spectra of: (A) nanoCHI and (B) nanoThioCHI.

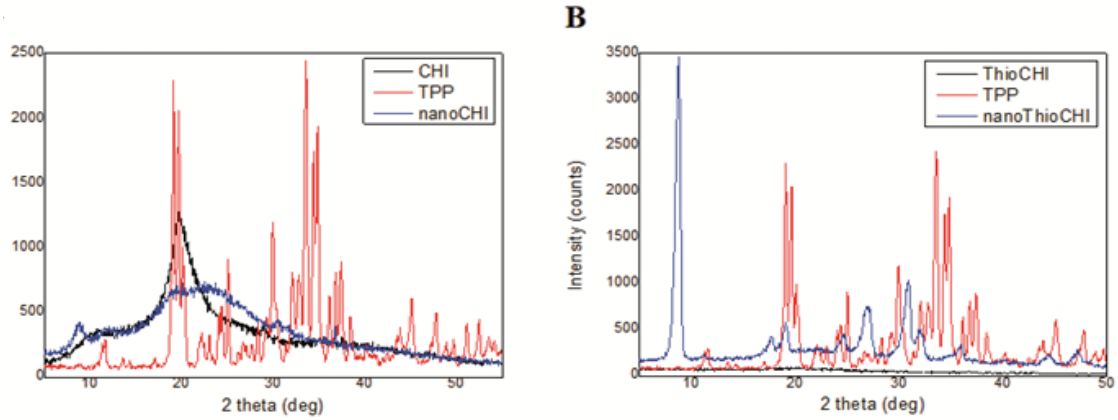

Fig. 2. XRD patterns of: (A) nanoCHI and (B) nanoThioCHI formulations

Concerning ThioCHI as was referred previously (Nanaki et al., 2017) is amorphous, with a broad peak be present in its X-ray diffraction (Fig. 2). The amorphization of ThioCHI is an indication that successful modification of CHI was conducted. Nanoparticles formed showed different characteristics. As it was observed ThioCHI nanoparticles showed a relative high crystallinity with a very high peak at 8.6 deg, i.e. at the same point where nanoCHI showed one also. There are other peaks at 17.7, 19.1, 24.6, 26.8, 30.9, 32.0, and 35.9 deg, at different degrees with that of TPP, indicating that the matrix formed is high crystalline. This observation is probably attributed to the modification in structure caused by the neutralization of pH after their initial formation. Esquivel et all (Esquivel et al., 2015) studied the influence of pH at nanoparticles formulation by ionic gelation technique using CHI and ThioCHI as polymers.

Concerning CHI nanoparticles it was found that when the pH was at the acidic region, and lower to 5.3 - a value near to pka of CHI, which is 6.5, smaller nanoparticles were formed and aggregation was not observed. This was found to be attributed to the protonation of amine groups (NH_3^+) that favors the extension of CHI free chains. As the pH increased near to isoelectric pH value, a deprotonation process occurred, leading to microaggregation by decreasing repulsion forces between particles. As SEM photos showed the proper attitude was also observed in our study. CHI nanoparticles formed (Fig. 3a) were spherical in shape, having size of about 380 nm, while after the adjustion of pH at 6.5 aggregates were observed (Fig. 3b). Analogous was the observation for ThioCHI nanoparticles formation which showed to be bigger in size, about 430nm, compared to nanoCHI (Fig. 3c) and spherical in structure and semispherical and aggregated at pH=6.5 (Fig. 3d).

Aggregations can lead to crystalline structures formation. The differences observed in XRD patterns concerning nanoformulation are probably ought to different mechanisms of formation. As was also referred in (Esquivel et al., 2015) nanoparticles are formed in two stages; at the first stage chitosan chains are arranged from semi coil state to expanded structure and at the second stage free CHI chains are reorganized to semispherical shapes. Furthermore, modification of CHI with thioglycolic acid affected structural reorganization ought to stereochemical inhibition.

Aiming the production of a final product of nanoparticles with enriched mucoadhesiveness, ThioCHI was selected as polymer for anti-VEGF encapsulation also based on its low cell cytotoxicity effect as shown by the cytotoxicity results below. SEM photo (Fig. 4) showed the successful preparation of the proper nanoparticles. As was expected, nanoparticles were smooth in surface but was agglomerated due to the last stage of neutralization process. Their size was bigger than that of net nanoThioCHI, showing that antibody was probably incorporated to the nanoparticles.

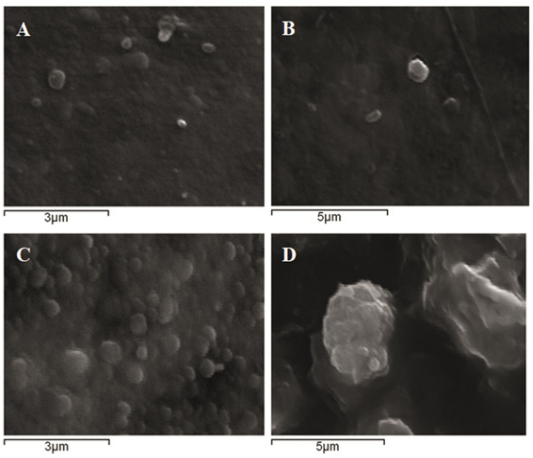

Fig. 3. SEM photos of nanoCHI and nanoThioCHI at pH 4 (A,B) and 6.5 (C,D) respectively.

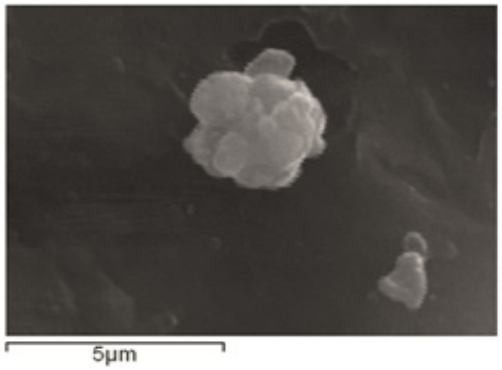

Fig. 4. SEM photo of nanoThioCHI containing antiVEGF

ASCs and HUVECs characterization

The successful isolation of a purified ASCs population was confirmed by flow cytometry for the absence of expression of hematopoietic markers (CD45 / CD34) and high co-expression percentage (approximately 88%) of CD90 / CD105 markers (Fig. 5a). The ability of ASCs to differentiate into adipocytes, osteocytes and chondrocytes was confirmed after staining with the appropriate dyes, compared with the control group that was not cultured in the presence of any differentiation medium and thus remained unstained (Fig. 5b).

We similarly confirmed the isolation of HUVECs both by flow cytometry for expression of endothelial markers (CD144 / CD146) and after observation of their morphology via optical microscopy (Fig. 6).

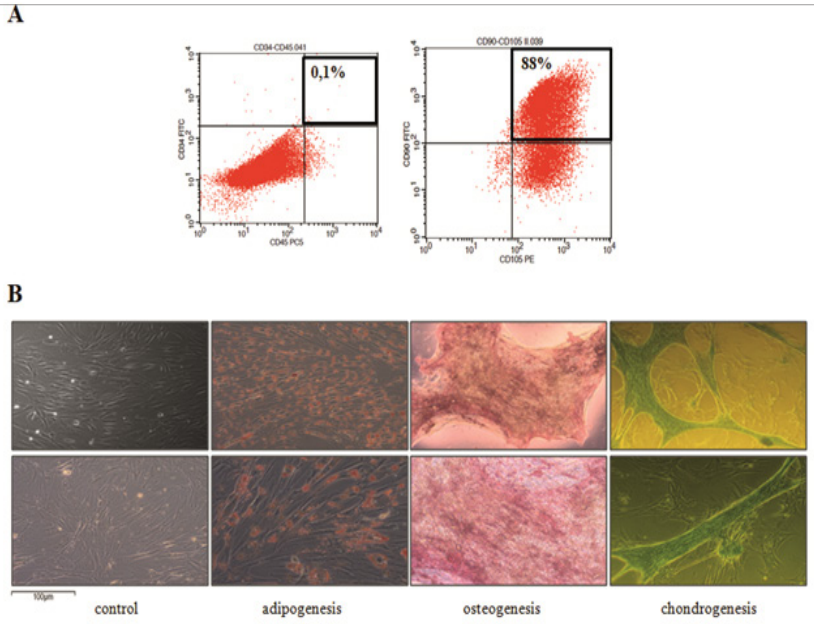

Fig.5. (A) Immunophenotypic characterization of isolated ASCs at passage 2 (B) Morphological depiction of ASCs differentiation capacity after specific staining towards adipocytes, osteocytes and chondrocytes in comparison with undifferentiated cells.

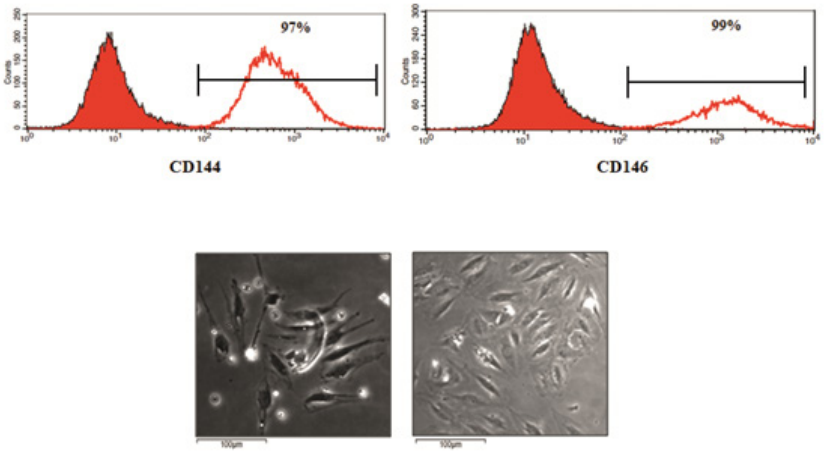

Fig. 6. (a) Immunophenotypic characterization of freshly isolated HUVEC (b) Morphological depiction of HUVEC after detachment on plastic surface.

Evaluation of the *in vitro* induced model of RVO

In order to induce toxicity to the selected endothelial cell line aiming the simulation of an *in vitro*RVO model, we gradually added increased concentrations of PD0325901 in the HUVEC cell line. We observed that the concentration of 500 μg MEK inhibitor per ml becomes statistically significant (**p = 0.0072) toxic with an observed decrease in HUVEC viability at 42.1%, similar to that of Triton-X-100 toxicity that was used as control group (Fig. 7a).

EPCR levels were measured at, the determined as cytotoxic, concentration of 500 μg / ml to confirm the toxic effect of PD0325901 on the endothelial cell line by enhancing the secretion of cytokines associated with RVO models. The statistically significant (**p = 0.006) overexpression of soluble EPCR relative to the untreated with the inhibitor-control group, implies the successful induction of the *in vitro* induced model (Fig. 7b). Moreover 24 and 48h upon PD0325901 stimulation, HUVECs express in high transcriptional levels the VEGF gene confirming that stressed endothelium also produces VEGF as a consequence of MEK inhibitor effect in the proposed model (Fig. 7c).

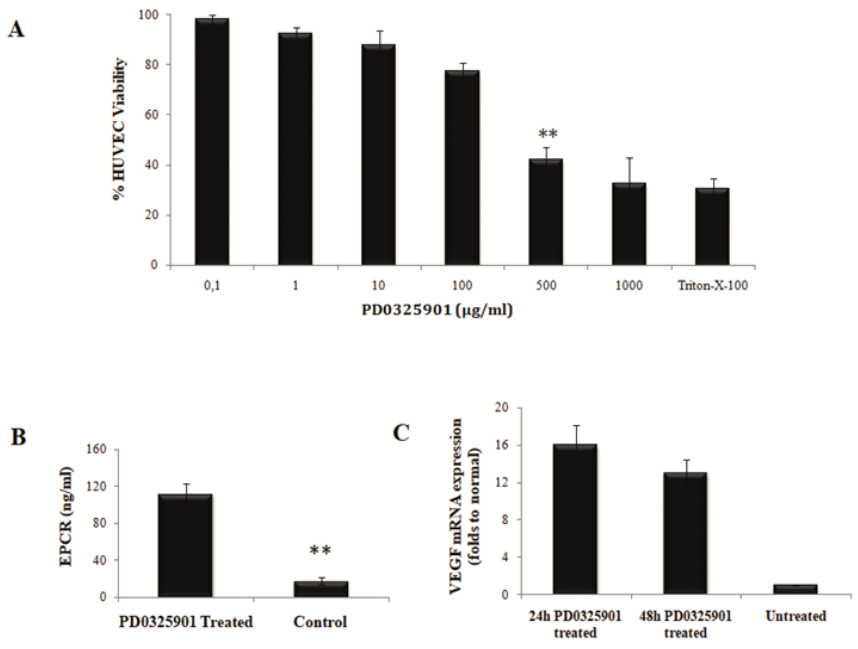

Fig. 7. Evaluation of the *in vitro* induced model of RVO (A) Quantification of PD0325901 toxicity on HUVECs viability with MTT assay (B) Determination of EPCR secretion levels from PD0325901-treated HUVECs (C) HUVECs' VEGF transcriptional level 24 and 48h upon PD0325901 stimulation. Data are expressed as the mean ±SD from four independent experiments (**p ≤ 0.01; n = 4).

Estimation of the cytotoxic effect of the prepared nanoparticles

The prepared chitosan and thiolated chitosan nanoparticles appeared not to be particularly toxic upon addition in ASCs cultures, even at high concentrations. In particular, nanoThioCHI appear to be safer than nanoCHI as they show cell viability levels similar to control group up to the concentration of 10 mg / ml (Fig. 8a). The observation of the morphology of the ASCs after the nanoparticles' effect confirms the MTT results with the maximum morphological apoptosis observed at the concentration of 20 mg / ml (Fig. 8b).

Given the fact that nanoThioCHI, which were prepared for this work aiming to enhance mucoadhesiveness and growth factors' bioavailability, present ideally lower cytotoxicity than nanoCHI, we continue the rest of our experiments by using only this category of modified chitosan's nanoparticles.

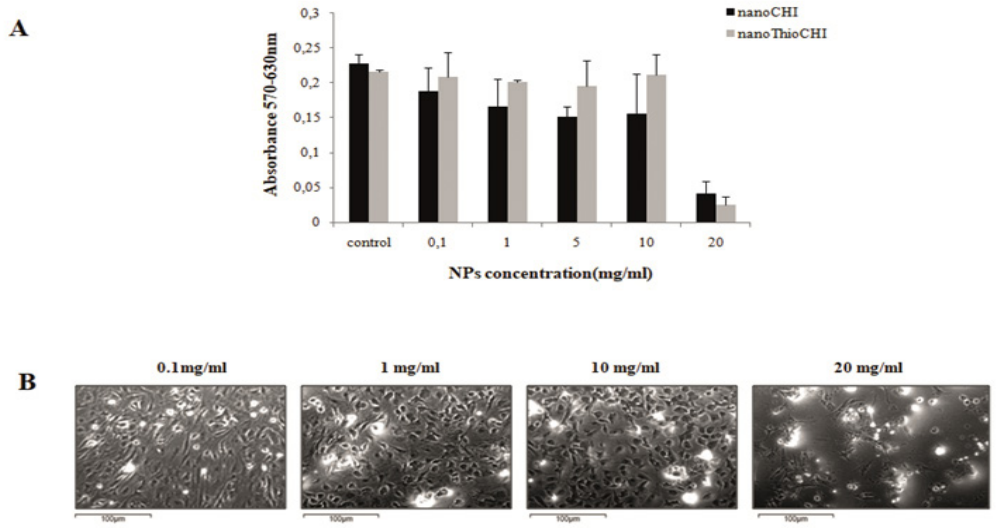

Fig. 8. (A) Determination of cell viability after the addition of increasing concentrations of nanoCHI and nanoThioCHI (n = 2) (B) Morphological observasion of cell cultures 24hours upon treatment with nanoThioCHI

Time-controlled release of encapsulated anti-VEGF

The quantification of the progressively increasing amount of secreted anti-VEGF from nanoThioCHI + anti-VEGF for 7 days, without temporary change of supernatant, confirms its time-controlled and sustained release (Fig. 9). The low secretion of anti-VEGF measured in the presence of nanoThioCHI, demonstrates that the amount of anti-VEGF that quantified is secreted by the nanoparticles in which it is encapsulated and not as cellular response to nanoparticles' addition in general.

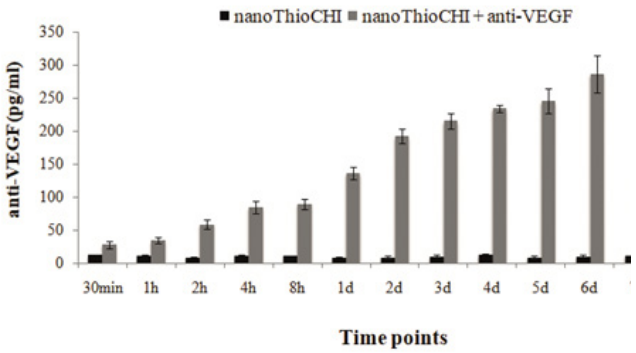

Fig. 9. Quantification of the released anti-VEGF from nanoThioCHI+anti-VEGF in 8days time period without medium change (n = 4).

Evaluation of the therapeutics influence on the *in vitro* induced RVO model

The decrease in the secretion levels of the RVO specific marker, EPCR, as a result of the presence of ASCs or their combination with nanoThioCHI+anti-VEGF in culture demonstrates their efficient activity. As we observed, the combination of cells and nanoparticles in the induced damage model, as depicted in Fig. 10a, contributes to a faster reduction of EPCR levels over a 24-hour period, as opposed to simply addition of ASCs only which approach respective expression levels one day later, at 48h (Fig. 10b). More specifically, the abnormal EPCR levels were statistically significantly reduced after 24 (*p = 0.04) and 48 (*p = 0.035) hours following exposure of the abnormal endothelium either to the nanoThioCHI+anti-VEGF or to ASCs. ASCs effect was statistically significant better at 48 hours. A combination of both agents was more effective than either agent separately on 24 (**p = 0.008) and (**p = 0.006).

Morphological observation of the cells' confluency demonstrates even after 48 hours and for all conditions that the above results are not affected by cells' viability reduction.

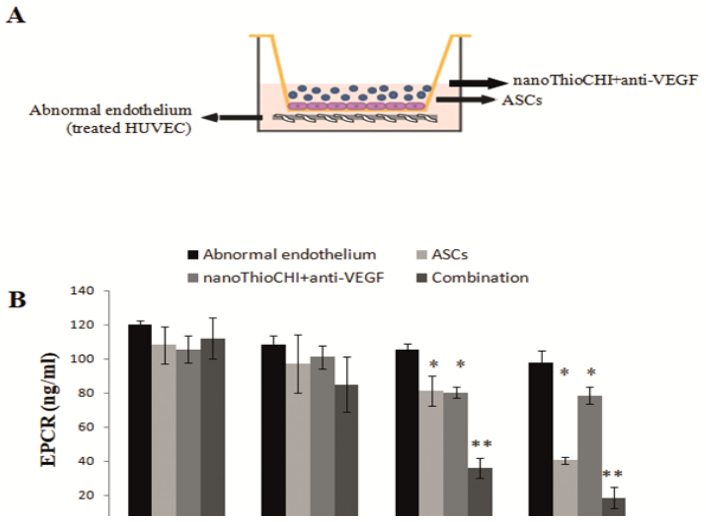

Fig.10. (A) Depiction of the designed coculture system aiming to test the result of ASCs/nanoThioCHI+anti-VEGF impact on the *in vitro* induced RVO model (B) Measurement of EPCR secreted levels from treated HUVEC as a response to combination exposure (*p < 0.05, **p < 0.01; n = 4)

Discussion

RVO is the fifth leading cause of blindness. Although it's exact pathophysiology and etiology remain unknown, it is generally accepted that the disease is related to conditions that cause endothelial dysfunction (Karia, 2010; Ponto et al., 2015; Kida, 2017) and is associated with increased risk of stroke (Li et al., 2016).

Innovative therapeutic approaches using intravitreal corticosteroids and anti-VEGF are currently studied in clinical trials (Bremond-Gignac, 2016), and at least two medicines containing anti-VEGF are FDA and EMA approved however the ideal therapeutic scheme remains to be determined (Campa et al., 2016). On the other hand novel therapeutic means such as MSCs may be also useful (Rajashekhar, 2014).

Huag et al (2009) have proposed the intravitreal administration of PD0325901 to Dutch-Belted Rabbits as a reliable pre-clinical experimental model of the disease (Huang et al., 2009). The same substance induces *in vitro* the release of sEPCR on endothelial cells (Huang et al., 2009). SEPCR has been also proposed as a disease marker for RVO (Gumus et al., 2006).

SEPCR binds to the activated protein C inhibiting its anticoagulative and antithrombotic activity (Liaw et al., 2000). Its release from endothelial cells can be considered as a stress marker of the endothelium (Saposnik et al., 2012) and a marker of hypercoagulation (Yilmaz et al., 2015). Accordingly the hypersecretion of sEPCR by HUVEC cells after PD0325901 stimulation as indicated by the results of the present study mimics the stressed vascular endothelium in RVO.

Furthermore, stressed endothelium produces also VEGF (Conklin et al., 2002; Dabagh et al., 2019), that plays a central role in RVO pathophysiology (Nishinaka et al., 2018). Accordingly, the results of the present paper indicate that PD0325901 stimulation induces VEGF expression on HUVEC cultures.

To our knowledge, this is the first use of a primary endothelial cell line for the induction of a PD0325901-mediated RVO model, enabling further investigation into the mechanisms underlying the disease induction system using this inhibitor.

The results of the present study indicate that augmented levels of secreted soluble EPCR were detected upon HUVECs' exposure to a cytotoxic dose of the inhibitor supporting its potential use as a biomarker for RVO. The soluble form of EPCR has recently been detected in RVO human plasma and in contrast to membrane-bound EPCR (CD201), plays a prothrombotic role by inhibiting protein C activation limiting the activation of anticoagulant pathway through the thrombin-thrombomodulin complex (Saposnik et al., 2004; Liaw et al., 2000). However, the mechanism by which PD0325901-induction of antioxidant genes leads to increase secretion of EPCR

remains to be clarified.

Having the above cell culture model of stressed endothelium, we attempted to test novel means of RVO therapy either separately or in combination.

It has been reported that the use of nanoparticles as the carriers for related to antiangiogenic therapy drugs, could effectively protect the drugs from inactivation, achieve sustained-release, controlled release and targeted drug delivery, significantly enhance the bioavailability and reduce the side effects (Lu et al., 2013; Wang et al., 2001). Polymeric nanoparticles are currently a promising candidate for ocular drug delivery because they are completely degradable, nontoxic and easy to be functionalized with various types of drugs Shen et al., 2011). Chitosan has already been used as a carrier for antibody delivery. Savin et al. (Savin et al., 2019) used chitosan grafted-poly (ethylene glycol) methacrylate for the near the retina delivery of bevacizumab (BEV), a full-length monoclonal VEGF antibody. It was found that this modality offered a prolonged local release up to 30 days, without showing any cytotoxicity. BEV was also studied (Ugurlu et al., 2019) as antibody and was successfully incorporated in chitosan nanoparticles prepared by ionic gelation.

Based on all the above, we here prepared for the first time a novel anti-VEGF nanocarrier of chitosan modified with thiol groups aiming the increase of its adhesiveness on the administration environment for locally targeted drug release. The data of the present study indicate that nanoThioCHI has no cytotoxic effect upon its addition in cell culture even in high concentrations while the respective anti-VEGF nanocarrier is capable of time-controlled and sustained release of the drug for 8 continuous days. This *in vitro* time period is likely to correspond to an in vivo time period greater than the already referred to the existed literature (Lu et al., 2013).

The paracrine properties of stem cells injected into the eye allow continuous secretion of neurotrophic, immunomodulatory, and anti-angiogenic factors that could potentially impact deteriorating retinal cells for a considerable period of time, with the advantage of superior potential than neurotrophic factors with a shorter half-lives and injected in a timely manner (Puertas-Neyra et al., 2020). For this reason, we here propose the combination of our prepared nanocarriers with a purified expanded and fully characterized ASCs' population as a potential therapeutic regimen against RVO and other related to retinal degeneration diseases.

Further research using an in vivo model of RVO, is required to verify the presented results and evaluate the efficacy of the proposed *in vitro* model.

Acknowledgments: The authors thank Biohellenika SA Biotechnology Company for providing the facilities and consumables that enabled the completion of this study.

Ευρωπαϊκή Ένωση
European Social Fund

Operational Programme
Human Resources Development, Education and Lifelong Learning
Co-financed by Greece and the European Union

ΕΣΠΑ 2014-2020
ανάπτυξη - εργασία - αλληλεγγύη

Funding: This research is co-financed by Greece and the European Union (European Social Fund- ESF) through the Operational Programme «Human Resources Development, Education and Lifelong Learning» in the context of the project "Strengthening Human Resources Research Potential via Doctorate Research" (MIS-5000432), implemented by the State Scholarships Foundation (IKY)

Compliance with ethical standards

Conflict of interest The authors declare that they have no conflict of interest.

Ethical approval This study was approved by the Ethics Committee of Aristotle University of Thessaloniki School of Medicine (390-9/1.7.2017).

Informed consent This research involves Human Participants after their informed consent.

Authors' contribution E.G. conceived the study; S.N. and D.B. fabricated and characterized the nanocarriers; E.G. and S.N. designed and performed the experiments; E.G., A.K., V.K., D.B. and G.K. analysed the data; E.G. and S.N. wrote the manuscript. All authors reviewed the manuscript.

References

1. Balmer, J., Stanzel, BV., Fischer, MD., 2015. Stem cell therapy for retinal diseases. Ophthalmologe. 112, 728–37. https://doi.org/10.1007/s00347-015-0119-2.

2. Bharti, K., Rao, M., Hull, SC., Stroncek, D., Brooks, BP., Feigal, E., et al., 2014. Developing cellular therapies for retinal degenerative diseases. Investig Ophthalmol. Vis. Sci. 55, 1191–201. doi:10.1167/iovs.13-13481.

3. Bremond-Gignac, D., 2016. Investigational drugs for retinal vein occlusion. Expert. Opin. Investig. Drugs. 25, 841–50. doi:10.1080/13543784.2016.1181750.

4. Campa, C., Alivernini, G., Bolletta, E., Battaglia Parodi, M., Perri, P., 2016. Anti-VEGF Therapy for Retinal Vein Occlusions. Curr. Drug. Targets. 17, 328–36. https://doi.org/10.2174/1573399811666150615151324.

5. Christodoulou, E., Nerantzaki, M., Nanaki, S., Barmpalexis, P., Giannousi, K., Dendrinou-Samara, C., et al., 2019. Paclitaxel magnetic core–shell nanoparticles based on poly(Lactic acid) semitelechelic novel block copolymers for combined hyperthermia and chemotherapy treatment of cancer. Pharmaceutics. 11. doi:10.3390/pharmaceutics11050213.

6. Conklin, BS., Zhong, DS., Zhao, W., Lin, PH., Chen, C., 2002. Shear

stress regulates occludin and VEGF expression in porcine arterial endothelial cells. J. Surg. Res. 102. 13–21. doi:10.1006/jsre.2001.6295.
7. Dabagh, M., Randles, A., 2019. Role of deformable cancer cells on wall shear stress-associated-VEGF secretion by endothelium in microvasculature. PLoS. One. 14. doi:10.1371/journal.pone.0211418.
8. Esquivel, R., Juárez, J., Almada, M., Ibarra, J., Valdez, MA., 2015. Synthesis and characterization of new thiolated chitosan nanoparticles obtained by ionic gelation method. Int. J. Polym. Sci. 2015. doi:10.1155/2015/502058.
9. Farjo, KM., Ma, JX., 2010. The potential of nanomedicine therapies to treat neovascular disease in the retina. J. Angiogenes. Res. 2. https://doi.org/10.1186/2040-2384-2-21.
10. Gumus, K., Kadayifcilar, S., Eldem, B., Saracbasi, O., Ozcebe, O., Dundar, S., et al., 2006. Is elevated level of soluble endothelial protein C receptor a new risk factor for retinal vein occlusion? Clin. Exp. Ophthalmol. 34, 305–11. doi:10.1111/j.1442-9071.2006.01212.x.
11. Huang, W., Yang, AH., Matsumoto, D., Collette, W., Marroquin, L., Ko, M., et al., 2009. PD0325901, a mitogen-activated protein kinase kinase inhibitor, produces ocular toxicity in a rabbit animal model of retinal vein occlusion. J. Ocul. Pharmacol. Ther. 25, 519–30. doi:10.1089/jop.2009.0060.
12. Inoue, Y., Iriyama, A., Ueno, S., Takahashi, H., Kondo, M., Tamaki, Y., et al., 2007. Subretinal transplantation of bone marrow mesenchymal stem cells delays retinal degeneration in the RCS rat model of retinal degeneration. Exp. Eye. Res. 85, 234–41. https://doi.org/10.1016/j.exer.2007.04.007.
13. Karia, N., 2010. Retinal vein occlusion: Pathophysiology and treatment options. Clin. Ophthalmol. 4, 809–16. doi:10.2147/opth.s7631.
14. Kida, T., 2017. Mystery of Retinal Vein Occlusion: Vasoactivity of the Vein and Possible Involvement of Endothelin-1. Biomed. Res. Int. 2017. doi:10.1155/2017/4816527.
15. Klein, R., Klein, BEK., Moss, SE., Meuer, SM., Gutman, FA., Ferris, FL., et al., 2000. The epidemiology of retinal vein occlusion: The beaver dam eye study. Trans. Am. Ophthalmol. Soc. 98, 133–43.
16. Koliakou, I., Gounari, E., Nerantzaki, M., Pavlidou, E., Bikiaris, D., Kaloyianni, M., et al., 2019. Differentiation Capacity of Monocyte-Derived Multipotential Cells on Nanocomposite Poly(e-caprolactone)-Based Thin Films. Tissue. Eng. Regen. Med. 16, 161–75. doi:10.1007/s13770-019-00185-z.
17. Li, M., Hu, X., Huang, J., Tan, Y., Yang, B., Tang, Z., 2016. Impact of retinal vein occlusion on stroke incidence: A meta-analysis. J. Am. Heart. Assoc. 5. doi:10.1161/JAHA.116.004703.
18. Liaw, PCY., Neuenschwander, PF., Smirnov, MD., Esmon, CT., 2000. Mechanisms by which soluble endothelial cell protein C receptor modulates protein C and activated protein C function. J. Biol. Chem. 275, 5447–52. doi:10.1074/jbc.275.8.5447.
19. Lu, Y., Zhou, N., Huang, X., Cheng, JW., Li, FQ., Wei, RL., et al., 2013. Effect of intravitreal injection of bevacizumab-chitosan nanoparticles on retina of diabetic rats. Int. J. Ophthalmol. 7, 1–7. doi:10.3980/j.issn.2222-3959.2014.01.01.
20. Mead, B., Berry, M., Logan, A., Scott, RAH., Leadbeater, W., Scheven, BA., 2015. Stem cell treatment of degenerative eye disease. Stem. Cell. Res. 14, 243–57. https://doi.org/10.1016/j.scr.2015.02.003.
21. Nanaki, S., Tseklima, M., Christodoulou, E., Triantafyllidis, K., Kostoglou, M., Bikiaris, DN., 2017. Thiolated chitosan masked polymeric microspheres with incorporated mesocellular silica foam (MCF) for intranasal delivery of paliperidone. Polymers (Basel). 9. doi:10.3390/polym9110617.
22. Nishinaka, A., Inoue, Y., Fuma, S., Hida, Y., Nakamura, S., Shimazawa, M., et al., 2018. Pathophysiological role of VEGF on retinal edema and nonperfused areas in mouse eyes with retinal vein occlusion. Investig. Ophthalmol. Vis. Sci. 59, 4701–13. doi:10.1167/iovs.18-23994.
23. Park, SS., 2016. Cell therapy applications for retinal vascular diseases: Diabetic retinopathy and retinal vein occlusion. Investig. Ophthalmol. Vis. Sci. 57. https://doi:10.1167/iovs.15-17594.
24. Ponto, KA., Elbaz, H., Peto, T., Laubert-Reh, D., Binder, H., Wild, PS., et al., 2015. Prevalence and risk factors of retinal vein occlusion: The Gutenberg Health Study. J. Thromb. Haemost. 13, 1254–63. doi:10.1111/jth.12982.
25. Puertas-Neyra, K., Usategui-Martín, R., Coco, RM., Fernandez-Bueno, I., 2020. Intravitreal stem cell paracrine properties as a potential neuroprotective therapy for retinal photoreceptor neurodegenerative diseases. Neural. Regen. Res. 15, 1631–8. doi:10.4103/1673-5374.276324.
26. Rajashekhar, G., 2014. Mesenchymal stem cells: New players in retinopathy therapy. Front. Endocrinol (Lausanne). 5. https://doi.org/10.3389/fendo.2014.00059.
27. Rajashekhar, G., Ramadan, A., Abburi, C., Callaghan, B., Traktuev, DO., Evans-Molina, C., et al., 2014. Regenerative therapeutic potential of adipose stromal cells in early stage diabetic retinopathy. PLoS. One. 9. https://doi:10.1371/journal.pone.0084671.
28. Saposnik, B., Peynaud-Debayle, E., Stepanian, A., Baron, G., Simansour, M., Mandelbrot, L., et al., 2012. Elevated soluble endothelial cell protein C receptor (sEPCR) levels in women with preeclampsia: A marker of endothelial activation/damage? Thromb. Res. 129, 152–7. doi:10.1016/j.thromres.2011.07.023.
29. Saposnik, B., Reny, JL., Gaussem, P., Emmerich, J., Aiach, M., Gandrille, S., 2004. A haplotype of the EPCR gene is associated with increased plasma levels of sEPCR and is a candidate risk factor for thrombosis. Blood.103, 1311–8. doi:10.1182/blood-2003-07-2520.
30. Savin, CL., Popa, M., Delaite, C., Costuleanu, M., Costin, D., Peptu, CA., 2019. Chitosan grafted-poly(ethylene glycol) methacrylate nanoparticles as carrier for controlled release of bevacizumab. Mater. Sci. Eng. C. 98, 843–60. doi:10.1016/j.msec.2019.01.036.
31. Senni, K., Pereira, J., Gueniche, F., Delbarre-Ladrat, C., Sinquin, C., Ratiskol, J., et al., 2011. Marine polysaccharides: A source of bioactive molecules for cell therapy and tissue engineering. Mar. Drugs. 9, 1664–81. https://doi.org/10.3390/md9091664.
32. Shen, HH., Chan, EC., Lee, JH., Bee, YS., Lin, TW., Dusting, GJ., et al., 2015. Nanocarriers for treatment of ocular neovascularization in the back of the eye: New vehicles for ophthalmic drug delivery. Nanomedicine. 10, 2093–107. doi:10.2217/nnm.15.47.
33. Siafaka, PI., Titopoulou, A., Koukaras, EN., Kostoglou, M., Koutris, E., Karavas, E., et al., 2015. Chitosan derivatives as effective nanocarriers for ocular release of timolol drug. Int. J. Pharm. 495, 249–64. doi:10.1016/j.ijpharm.2015.08.100.
34. Ugurlu, N., Aşık, MD., Çakmak, HB., Tuncer, S., Turk, M., Çagıl, N., et al., 2019. Transscleral delivery of bevacizumab-loaded chitosan nanoparticles. J. Biomed. Nanotechnol. 15, 830–8. doi:10.1166/jbn.2019.2716.
35. Wang, JJ., Zeng, ZW., Xiao, RZ., Xie, T., Zhou, GL., Zhan, XR., et al., 2011. Recent advances of chitosan nanoparticles as drug carriers. Int. J. Nanomedicine. 6, 765–74. doi:10.2147/ijn.s17296.
36. Xian, X., Gopal, S., Couchman, JR., 2010. Syndecans as receptors and organizers of the extracellular matrix. Cell. Tissue. Res. 339, 31–46. https://doi.org/10.1007/s00441-009-0829-3.
37. Xu, W., Xu, GX., 2014. Mesenchymal stem cells for retinal diseases. Int. J. Ophthalmol. 4, 413–21. https://doi:10.3980/j.issn.2222-3959.2011.04.19.
38. Xu, Y., Du, Y., 2003. Effect of molecular structure of chitosan on protein delivery properties of chitosan nanoparticles. Int. J. Pharm. 250, 215–26. https://doi.org/10.1016/S0378-5173(02)00548-3.

39. Yilmaz, H., Cakmak, M., Inan, O., Darcin, T., Aktas, A., Gurel, OM., Bilgic, MA., Bavbek, N., Akcay, A., 2015. Association of ambulatory arterial stiffness index with sEPCR in newly diagnosed hypertensive patients. Ren. Fail. 37, 1409–13. doi:10.3109/0886022X.2015.1074472
40. Zhao, LM., Shi, LE., Zhang, ZL., Chen, JM., Shi, DD., Yang, J., et al., 2011. Preparation and application of chitosan nanoparticles and nanofibers. Brazilian. J. Chem. Eng. 28, 353–62. https://doi.org/10.1590/S0104-66322011000300001.
41. Zhu, X., Su, M., Tang, S., Wang, L., Liang, X., Meng, F., et al., 2012. Synthesis of thiolated chitosan and preparation nanoparticles with sodium alginate for ocular drug delivery. Mol. Vis. 18, 1973–82.